Design and Analysis of Trench Assisted Large Mode Area Leaky Channel Waveguide for High-Power Applications

A Dissertation submitted towards the partial fulfillment of

the requirement for the award of degree of

Master of Technology

In

Nanoscience and Technology

Submitted By

Sandeep Singh

2K11/NST/14

Under the supervision of

Dr. Ajeet Kumar

(Assistant Professor)

Department of Applied Physics

Delhi Technological University

(Formerly Delhi College of Engineering)

CERTIFICATE

This is to certify that the dissertation title **"Design and Analysis of Trench Assisted Large Mode Area Leaky Channel Waveguide for High-Power Applications"** is the authentic work of **Mr. Sandeep Singh** under my guidance and supervision in the partial fulfillment of requirement towards the degree of Master of Technology in **Nanoscience and Technology**, run by the Dept. of Applied Physics in **Delhi Technological University.**

Dr. Ajeet Kumar	Prof.S.C.Sharma
Supervisor	HOD
Assistant Professor	Deptt. of Applied Physics
Delhi Technological University	Delhi Technological University

DECLARATION BY THE CANDIDATE

I hereby declare that the work presented in this dissertation entitled "**Design and Analysis of Trench Assisted Large Mode Area Leaky Channel Waveguide for High-Power Applications**" has been carried out by me under the guidance of Dr. Ajeet Kumar, Assistant Professor, Department of Applied Physics, Delhi Technological University, Delhi and hereby submitted for the partial fulfillment for the award of degree of Master of Technology in Nanoscience and Technology at Applied Physics Department, Delhi Technological University, Delhi.

I further undertake that the work embodied in this major project has not been submitted for the award of any other degree elsewhere.

Sandeep Singh

2K11/NST/14

M.Tech (NST)

ACKNOWLEDGEMENT

I am indebted to my thesis supervisor **Dr. Ajeet Kumar**, Department of Physics, for his gracious encouragement and very valued constructive criticism that has driven me to carry the project successfully.

I am deeply grateful to **Prof. S.C.Sharma**, Head of Department (Applied Physics), Delhi Technological University for his support and encouragement in carrying out this project.

I wish to express my heart full thanks to my branch coordinator **Prof. Pawan Kumar Tyagi** and friends for their goodwill and support that helped me a lot in successful completion of this project.

This project wouldn't have been completed without the sincere help of research scholar **Mr. Than Singh Saini.**

I express my deep sense of gratitude to my parents **Mr.Kamalesh Singh, Mrs.Nirmala Singh** and to my elder sister and brother.

Finally I would like to thank almighty God for his blessings without which nothing is possible in this world.

Sandeep Singh
M.Tech (Applied Physics)
2k11/NST/14

Table of Contents

List of Figures

ABSTRACT

Integrated-optic waveguide lasers have drawn considerable attention for their compactness and possibility of device integration. A lot of interest has been shown to increase the mode area of waveguide for applications in optical communication and high-power laser and amplifier. For waveguide laser and amplifier applications, it is preferable to use a waveguide that supports only one mode to avoid instability arising from intermodal dispersion and mode competition. A conventional single-mode waveguide has a small guiding core. The tight light confinement in such a waveguide can reduce the optical damage threshold of the waveguide and at the same time, give rise to significant nonlinear optical effects, which limit ultimately the power handling capability of the waveguide.

A preferred structure for high-power applications should be one that has a large core and yet supports only a single mode. Here a novel cladding design in which the refractive index is uniform but the geometry is so designed that all the modes are leaky. Such a geometrically shaped cladding is highly dispersive and can also lead to single-mode operation over an extended range of wavelengths. Using properly chosen parameters, the waveguide can exhibit single-mode operation in the wavelength range 900–1600nm with a large core area.

Chapter 1

INTRODUCTION

Integrated Optics [1] is a new and exciting field of activity which is primarily based on the fact that light can be guided and confined in very thin films (with dimensions– wavelength of light) of transparent materials on suitable substrates. By a proper choice of substrates and films and a proper configuration of the waveguides, one can perform a wide range of operations such as modulation, switching, multiplexing, filtering or generation of optical waves. Due to the miniature size of these components, it is possible to obtain a high density of optical components in space unlike the case in bulk optics. These devices are expected to be rugged in construction, have good mechanical and thermal stability, be mass producible with high precision and reproducibility, and have small power consumption.

One of the most promising applications of integrated optics is expected to be in the field of optical fibre communications. The field of optical fibre communication has assumed tremendous importance because of its high information – carrying capacity. Integrated optics is expected to play an important role in optical signal processing at the transmitting and receiving ends and on regeneration at the repeaters. Other important applications of integrated optics are envisaged to be in spectrum analysis and optical signal processing.

In addition to the above, use of integrated optic techniques may lead to the realization of new devices which may be too cumbersome to be fabricated in bulk optics. The very high concentration of energy in very small regions in the optical waveguide leads to enormous intensities leading to the realization of nonlinear devices employing second harmonic generation etc. The confinement of light energy in small regions of space also leads to an efficient interaction of the optical energy with an applied electric field or an acoustic wave, thus leading to much more efficient electro-optic and acousto-optic modulators and deflectors requiring very low drive powers.

The goal of integrated optics (IO) is to develop miniaturized optical devices of high functionality on a common substrate. The state-of-the-art of integrated optics is still far

behind its electronic counterpart. Today, only a few basic functions are commercially feasible. However, there exists a growing interest in the development of more and more complex integrated optical devices.

In IO, we distinguish between **optical integrated circuits**, which perform functions similar to electronic circuits in communications systems, and **planar optical devices**, which are integrated optical systems other than communication systems.

1.1 Optical Integrated Circuits

Researchers hope to put waveguides, modulators, switches, and other active optical functions onto various substrates. It is visualized that thin films and micro-fabrication technologies can suitably be adopted to realize optical counterparts of integrated electronics for signal generation, modulation, switching, multiplexing and processing.

In optical integrated circuits, light is confined in thin film wave guides that are deposited on the surface or buried inside a substrate. Glasses, dielectric crystals and semiconductors can be used as substrate materials. The functions that can be realized depend on the type of substrate used. Researchers are challenged to identifying materials which have both the right electro-optical properties and a reliable means of forming them into useful structures on the integrated circuit. Unfortunately, many current-generation materials that are used to fabricate monolithic optical devices have high attenuation and therefore high transmission losses.

The most fundamental building block of an optical integrated circuits is a **channel wave guide** [2]. Wave guides in integrated-optics work similar to conventional fibers, trapping light in a length of material. This material is surrounded by material of a different index of refraction. The waveguides are made either by depositing material on top of a substrate and etching unwanted portions away, or etching trenches in the substrate and fillingssss them with polymers, silicates, or other light-transmitting materials.

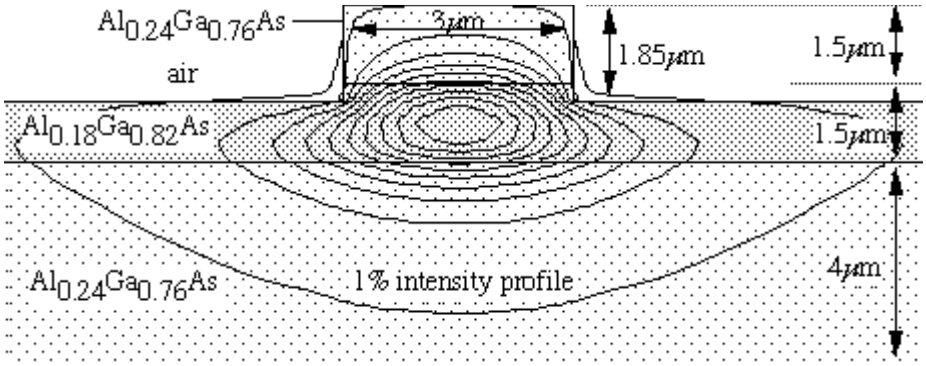

Figure 1.1 Typical structure of channel waveguide

(Source- Fundamentals of Integrated Optical Waveguides : Alejandro Martinez)

The basic requirements of a thin film optical guide material are that it is transparent to the wavelength of interest and that it has a refractive index higher than that of the medium in which it is embedded.

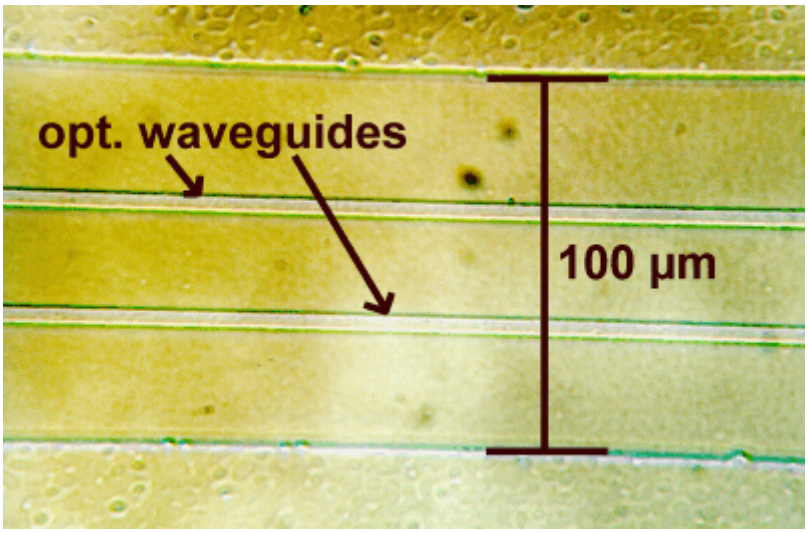

Figure 1.2 optical waveguide

(Source- Fundamentals of Integrated Optical Waveguides : Alejandro Martinez)

Within an optical integrated circuit, light propagates as a guided wave in a dielectric thin film. Appropriate addition of functional devices between interconnecting wave guides enables the realization of an optical integrated circuit for a specific use.

Some devices can be made on planar substrates using standard lithographic processes and thin-film technologies. Electron beam writing and laser beam writing are increasingly employed to produce patterns with high resolution. Epitaxial methods are used in the fabrication of sources, detectors and opto-electronic circuits on GaAs, Si and InP.

For a square channel waveguide of depth d the number of modes is approximately m^2, where $m = (2d/\lambda)$ NA, $m >> 1$. For a slab wave guide the number of modes is approximately m. For single mode operation in any channel wave guide we therefore need $(2d/\lambda)*NA \leq 1$, where d is the width of the channel. A single mode wave guide can be constructed by making d and NA sufficiently small. NA is the numerical aperture and for small Δ is given by $NA = n_{core}(2\Delta)^{1/2}$, where $\Delta = (n_{core} - n_{cladding})/n_{core}$.

In integrated optics, two main kinds of waveguides are used; these are the Planar and Strip guides. In planar waveguides, the confinement of the light energy is only along one transverse dimension and the light energy can diffract in the other transverse dimension .In constrast to planar waveguides, strip waveguides confine the light energy in both transverse dimensions; this confinement is a desirable feature for the fabrication of devices such as amplitude or intensity modulators, directional couplers, optical switches etc.

1.2 Optical Integrated Waveguide

An optical waveguide is a physical structure that guides electromagnetic waves in the optical spectrum. Common types of optical waveguides include optical fiber and rectangular waveguides.

Optical waveguides are used as components in integrated optical circuits or as the transmission medium in local and long haul optical communication systems. Optical waveguides can be classified according to their geometry (planar, strip, or fiber waveguides), mode structure (single-mode, multi-mode), refractive index distribution (step or gradient index) and material (glass, polymer, semiconductor).

An optical waveguide is a spatially inhomogeneous structure for guiding light, i.e. for restricting the spatial region in which light can propagate. Usually, a waveguide contains a region of increased refractive index, compared with the surrounding medium

(called *cladding*). However, guidance is also possible, e.g., by the use of reflections, e.g. at metallic interfaces. Some waveguides also involve plasmonic effects at metals.

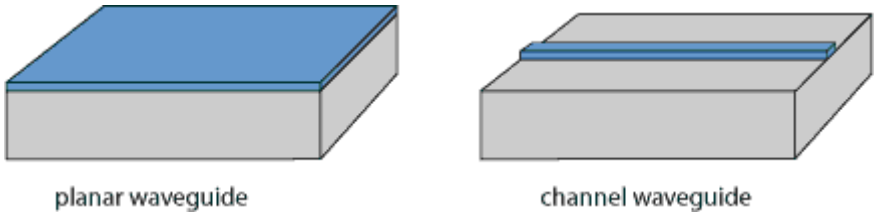

Fig.1.3: Two different kinds of waveguides. Planar waveguides guide light only in the vertical direction, whereas channel waveguides guide in two dimensions.

(Source- Fundamentals of Optical Waveguides: Katsunari Okamoto)

Most waveguides exhibit two-dimensional guidance, thus restricting the extension of guided light in two dimensions and permitting propagation essentially only in one dimension. An example is the *channel waveguide* shown in Figure 1.3. The most important type of two-dimensional waveguide is the optical fiber. There are one-dimensional waveguides, often called planar waveguides.

1.3 Planar (Slab) Waveguides

- An optical waveguide is characterized by light confinement in two dimensions and guiding along the third dimension.
- As a starting approach, the problem can be simplified if we consider only confinement in one dimension.
- This is the case of the structure known as planar or slab waveguide, which is also used as a intermediate structure to model and implement optical integrated waveguides.
- The slab waveguide consists of three layers of materials with different dielectric constants, extending infinitely in the directions parallel to their interface

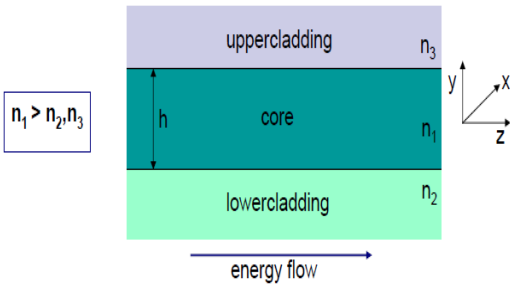

Fig.1.4 Structure of Planar Slab Waveguide

(Source- Fundamentals of Optical Waveguides: Katsunari Okamoto)

1.4 Channel Waveguides

- A channel waveguide (with guidance in both directions) has a guiding structure in the form of a stripe with a finite width.
- This may be a ridge on top of the cladding structure or an embedded channel. The latter has more symmetric waveguide modes.
- They are extensively used, for example, within various laser diodes. Small, low-power LDs have a single-mode channel waveguide with transverse dimensions of, for example, 1µm. Broad area LDs have a wider channel that supports multiple modes in the horizontal direction. Diode bars (diode arrays) contain an array of broad-stripe diode structures.

Fig.1.5 Channel waveguide

(Source- Fundamentals of Optical Waveguides: Katsunari Okamoto)

Larger channel and planar waveguides made from rare earth doped dielectric materials are used for high-power waveguide lasers and amplifiers. Pump light may be injected along the amplified beam, from the side, or from the top. Even in situations with strong heating, the waveguide may help to stabilize a single-mode laser beam with high beam quality.

1.5 Channel Waveguide Types

The second important system of integrated optics arises when the waveguides take the form of channel guides. These still lie on a planar substrate, but are now arranged to confine the optical field in two directions, x and y. Figure 1.6-1 shows cross sections through the most common geometries.

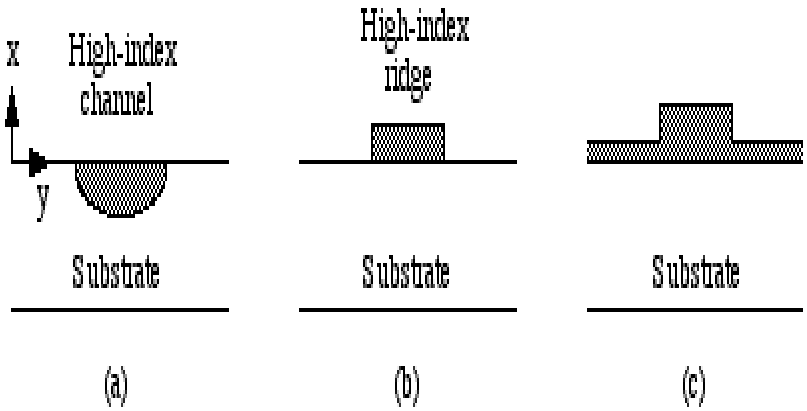

Figure 1.6-1 Channel waveguide types: a) buried, b) ridge and c) strip-loaded.

(Source- Fundamentals of Optical Waveguides: Katsunari Okamoto)

1) Buried Channel Guides

Figure 1.6-1a shows a buried channel guide, which is made by modifying the properties of the substrate material so that a higher refractive index is obtained locally. Most fabrication processes result in a weak, graded-index guide buried just below the surface, and, although channel guides normally have one axis of symmetry, they usually lack a well defined cross-sectional shape.

Diffusion is often used to fabricate guides of this type. For example, titanium metal can be diffused into lithium niobate or lithium tantalate substrates, by first depositing the metal in patterned strips of ≈1000 Å thickness and then carrying out an in-diffusion at a high temperature (≈1000ºC) for several hours (3 to 9). This is known as the Ti:$LiNbO_3$ process. The additional impurities cause a change in refractive index that is approximately proportional to their concentration, with a typical maximum value of $\Delta n = 0.01$. Figure 1.7 shows contours of constant refractive index that are obtained by diffusion of Ti metal into $LiNbO_3$.

Alternatively, material can be exchanged with the substrate. For example, protons (H+ ions) can be exchanged with Li+ ions in $LiNbO_3$. This is done by first covering the substrate with a masking layer, which is patterned so narrow stripe openings are made. The crystal is then placed in a suitable hot melt (in this case, benzoic acid, heated to ≈200ºC), and exchange of material takes place through the crystal surface in regions exposed by the mask openings. Proton exchange yields an index change of $\Delta n = +0.12$ for one polarization mode (the TM mode), but the index change is actually negative for the other one. Consequently, a waveguide is only formed in the former case. Silver ions can be exchanged with Na+ ions in soda-lime glass in a similar way, by immersing the substrate in molten $AgNO_3$, at temperatures of 200 - 350ºC. In this case, the time required to form a guide is large several hours), but if a DC electric field is used to assist the ion migration, the process can be speeded up quite considerably. The index change obtained is $\Delta n = 0.1$.

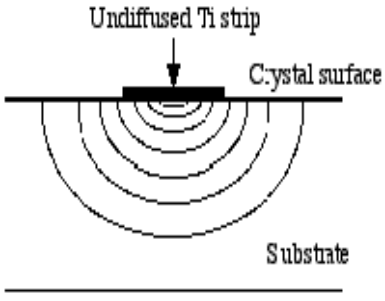

Figure 1.7 Contours of constant refractive index in a Ti-diffused channel waveguide.

(Source- Fundamentals of Optical Waveguides: Katsunari Okamoto)

2) Ridge Waveguides

Figure 1.6-1b shows a ridge waveguide. This is a step-index structure, usually fabricated from a planar guide that has been patterned and etched to leave a ridge. Total internal reflection then takes place at the sides of the guide, as well as the top and bottom faces. Often, the etching is designed to follow specific crystal planes, so the edges of the ridge may be sloped. Similarly, material is often (especially in laser structures) regrown around the sides of the guide. Much higher field confinement is possible using a ridge than a buried guide. As mentioned above, the index change that can be obtained by material modification is very small, so the evanescent field of any guided mode must extend for some distance outside the core. In a ridge guide, on the other hand, there can be a large index difference between the ridge and its surround. This is an important advantage; for example, bends can be much tighter in ridge-guide systems. Waveguides are often made as ridges in semiconductor materials, because of the ease with which a mesa structure may be made by etching. There are two: heterostructure guides, which operate by the refractive index differences obtained between different materials, and homostructure guides, which use the index reduction following from an increase in the majority carrier density.

The two most common semiconductor materials used in optoelectronics are based on the ternary alloy gallium aluminium arsenide and the quaternary alloy indium gallium arsenide phosphide, respectively. To fabricate heterostructure waveguides in the GaAs/GaAlAs system, successive layers of material are first grown on a GaAs substrate, in differing compositions of the general form $Ga_{1-x}Al_xAs$ (where x is the mole fraction of the constituent). Because GaAs and GaAlAs have similar lattice parameters, these additional layers are lattice-matched to the substrate and the composite crystal can grow without strain.

For example, Figure 1.8 shows how a planar guide might be fabricated using a layer of high-index GaAs, grown epitaxially on top of a thick layer of $Ga_{1-x}Al_xAs$ (which acts as a low-index isolation layer, separating the guide from the high-index GaAs substrate). The guiding layer may then be etched down to a narrow rib, to form a ridge guide.

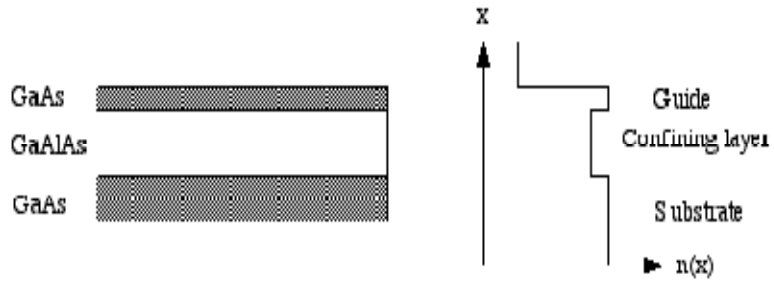

Figure 1.8 A GaAs/GaAlAs planar waveguide.

(Source- Fundamentals of Optical Waveguides: Katsunari Okamoto)

Waveguide fabrication is similar in the InP/InGaAsP system. This time, layers of the quaternary alloy $In_{1-x}Ga_xAs_{1-y}P_y$ are grown on an InP substrate. However, lattice-matching to the substrate is only obtained for particular combinations of x and y. More complicated layered structures are also often used. For example, Figure 1.9 shows a double heterostructure waveguide, which has a low-index GaAlAs confining layer on both sides of the guide. This arrangement is used extensively in semiconductor lasers, since the difference in bandgap between the GaAs and GaAlAs layers can provide carrier confinement in addition to confinement of the optical field.

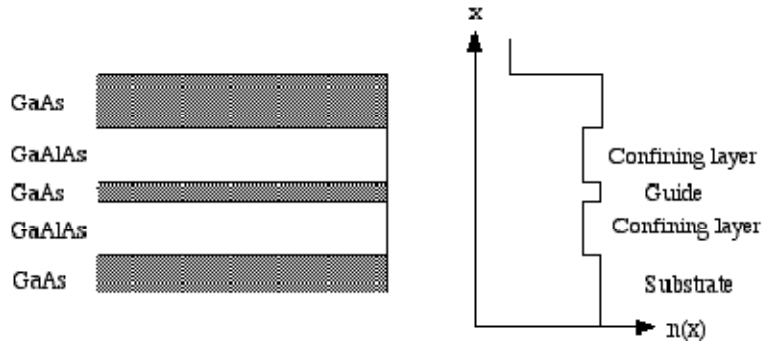

Figure 1.9 A double heterostructure GaAs/GaAlAs planar waveguide.

(Source- Fundamentals of Integrated Optical Waveguides : Alejandro Martinez)

Alternatively, a similar structure may be created by proton bombardment of an n-type substrate. This creates damage sites near the surface, which trap free carriers. This is known as free carrier compensation, and produces a increase in refractive index. The index change obtained by doping may be found for n-type GaAs as $\Delta n = -0.01$, when $N = 5\times10^{18}$ cm^{-3} and $\lambda_0 = 1$ μm. This implies that the index changes possible in

homostructures are much lower than in heterostructures, giving reduced confinement in any guide structure. In fact, since $m_h^* \gg m_e^*$ in InP, the hole-induced index difference is much smaller than the equivalent electron-induced value, so only n-type material is useable for waveguiding. A further problem arising in homostructures is that the increased carrier concentration in the substrate causes a rise in absorption, which can result in unacceptable propagation loss. Heterostructures therefore offer several advantages.

Ridge guides can also be made in amorphous material on semiconducting substrates. One common system involves silicon oxynitride guides, constructed on a silicon dioxide buffer layer, which in turn lies on a silicon substrate. Silicon oxynitride has a relatively high refractive index, but one which is lower than that of the silicon, for which $n = 3.5$. The two are therefore separated by a thick layer of SiO_2, which acts as a low-index ($n = 1.47$) spacer. Other systems use doped silica (e.g. an SiO_2/TiO_2 mixture) on top of the silica buffer layer. These are important, since they allow the fabrication of waveguides in a form compatible with VLSI electronics.

3) Strip-Loaded Waveguides

Two-dimensional confinement may also be less obvious. Figure 1.6c shows a strip loaded guide. Here, a three-layer structure has been used, which has a substrate, a planar layer, and then a ridge. The planar layer is arranged as a guide, but one that is just cut off. However, the addition of a further high-index overlay is sufficient to induce guiding in a localised region near the ridge. Confinement of the optical field in the y-direction is obtained because the refractive index, when averaged in the x-direction, is higher in the region of the ridge. The additional ridge overlay may have a different refractive index to that of the planar guide, or the same index.

1.5 Objectives and Organization of the Thesis

This thesis is concerned with the design of Large-core single-mode trench assisted leaky channel waveguide for high-power applications**.** A large-mode-area design in channel waveguide is presented for extended single-mode operation. Proposed design is characterized by a rectangular core and trench assisted cladding. Overall design is leaky and supports a finite leakage loss to all the modes of waveguide. The design works on the principle of **mode filtering**. The thesis consists of five chapters. This dissertation

has been ordered in such a way that the process of constructing the proposed design is evident throughout.

Chapter 2 introduces the speciality optical fibers and waveguides.

Chapter 3 deals with the Method of Analysis which includes Effective-index method and Transfer Matrix method for the analysis of Leaky channel waveguide.

Chapter 4 presents the result and analysis of proposed design for high-power applications.

Chapter 5 presents the concluding remarks and scope for the future work.

Chapter 2

Specialty Optical Fiber and Waveguides

The dramatic reduction of transmission loss in optical fibers coupled with equally important developments in the area of light sources and detectors has brought about a phenomenal growth of the fiber optic industry during the past two decades. The birth of optical fiber communication coincided with the fabrication of low-loss optical fibers and room-temperature operation of semiconductor lasers in 1970. Ever since, the scientific and technological progress in this field has been so phenomenal that we are already in the fifth generation of optical fiber communication systems within a brief span of 30 years. Recent developments in optical amplifiers and wavelength division multiplexing (WDM) are taking us to a communication system with almost “zero” loss and “infinite” bandwidth. Indeed, optical fiber and waveguide based communication systems are fulfilling the increased demand on communication links, especially with the proliferation of the Internet. This module, **Optical Waveguides and Fibers** [4] , is an introduction to the basics of fiber optics and waveguide network, discussing especially the characteristics of optical fibers and waveguides as regards their application to telecommunication

The introduction of wavelength division (WDM) technology put even greater demands on fiber design and composition to achieve wider bandwidth and flat gain. Efforts to extend the bandwidth of erbium doped fibers and develop amplifiers at other wavelength such as 1300 nm have spurred development of other dopants. Doping with ytterbium (Yb) allows pumping from 900 to 1090 nm using solid –state lasers or Nd and Yb fiber lasers. Of recent interest is the ability to pump Er/Yb fibers in a double-clad geometry with high power sources at 920 or 975 nm. Double-clad fibers are also being used to produce fiber lasers using Yb and Nd. Besides the amplification fiber, the erbium-doped amplifier requires a number of optical components for its operation. These include wavelength multiplexing and polarization multiplexing devices for the pump and signal wavelengths. Filters for gain flattening, power attenuators, and taps for power monitoring among other optical components are required for module performance. Also, because the amplifier enabled transmission distances of hundreds of kilometeres without regeneration, other propagation properties became important.

These properties include chromatic dispersion, polarization dispersion, and nonlinearities such as four-wave mixing (FWM), self- and cross-phase modulation, and Raman and Brillouin scattering. Dispersion compensating fibers were introduced in order to deal with wavelength dispersion. Broadband compensation was possible with specially designed fibers. However, coupling losses between the transmission and the compensating fibers was an issue. Specially designed mode conversion or bridge fibers enabled low-loss splicing among these three fibers, making low insertion loss dispersion compensators possible. Fiber components as well as micro optic or in some instances planar optical components can be fabricated to provide for these applications. Generally speaking, but not always, fiber components enable the lowest insertion loss per device. A number of these fiber devices can be fabricated using standard SMF, but often special fibers are required. Specialty fibers are designed by changing fiber glass composition, refractive index profile, or coating to achieve certain unique properties and functionalities. In addition to applications in optical communications, specialty fibers find a wide range of applications in other fields, such as industrial sensors, biomedical power delivery and imaging systems, military fiber gyroscope, high power lasers. A few such fibers are described in the following.

2.1. Bragg Fibers

Bragg fibers [5] were proposed theoretically as early as in 1978, but only recently have such structures been demonstrated. Since then, they have attracted much attention, mainly because they offer the possibility of air guiding. Some important advantages of air core fibers are the possibility of reducing propagation loss below the level of 0.2 dB/km (the value of current telecommunication fibers), and the greatly increased power threshold for the onset of nonlinear optical phenomena such as stimulated Raman scattering. The air core fibers in the literature can be roughly classified in two categories, (i) Bragg fibers, where the air core is surrounded by cylindrical dielectric layers with alternating refractive indices, and (ii) photonic crystal fibers (PCF) [6], where the fiber cladding is composed of a two dimensional (2D) array of air holes. PCFs are typically based on silica glass, which has excellent material properties and forms the backbone of modern optical telecommunications, whereas current air core Bragg fibers are based on a combination of polymer and soft glass. Fiber Bragg gratings (FBGs) [7] are spectral filters fabricated within segments of optical fiber. They typically

reflect light over a narrow wavelength range and transmit all other wavelengths, but they also can be designed to have more complex spectral responses. Many uses exist for FBGs in today's fiber communications systems, which rely heavily on dense wavelength division multiplexing (WDM), and optical amplification.

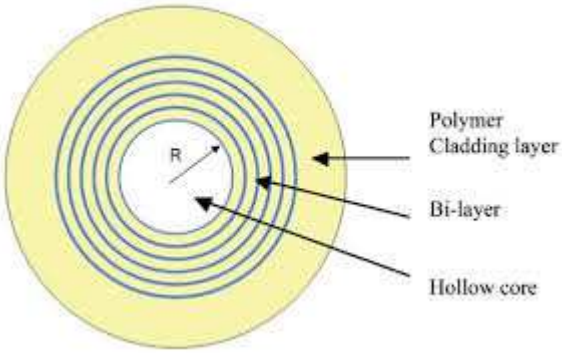

Figure 2.1. Schematic diagram of a Bragg fiber

(Source- T.S. Saini, A. Kumar, V. Rastogi and R. K. Sinha, "Multi-trench Channel Waveguide for Large-Mode-Area Single-Mode Operation,'')

FBGs are based on the principle of Bragg reflection. When light propagates through periodically alternating regions of higher and lower refractive index, it is partially reflected at each interface between those regions. If the spacing between those regions is such that all the partial reflections add up in phase i.e. when the round trip of the light between two reflections is an integral number of wavelengths, the total reflection can grow to nearly 100% , even if the individual reflections are very small. Of course, that condition will only hold for specific wavelengths. For all other wavelengths, the out of phase reflections end up canceling each other, resulting in high transmission.

To create the appropriate stack of high and low- refractive-index regions along a piece of optical fiber, manufacturers must permanently modify the refractive index of the fiber via the photosensitive effect. This is accomplished by exposing the optical fiber to ultraviolet (UV) light wth a wavelength around 240 nm or less. The photosensitivity is primarily due to the germanium dopant used in the core of most commercial fibers. Photosentivity can be increased by raising the germanium doping level, or by in-diffusing molecular hydrogen, which acts as a catalyst to the reaction of the germanium with UV light and greatly reduces exposure time. The index change is very stable, even

at high temperatures, especially if the grating is preannealed (heated to a temperature between 150º C and 500º C after fabrication). The fabrication itself is a simple four step process: Remove the acrylate coating, expose the fiber to UV light, preanneal, and then recoat the fiber. To create a Bragg grating in an optical fiber, one needs to generate the required periodic pattern of UV light on the side of the fiber. This can be done by splitting a UV laser beam and recombining it in the fiber to form a standing wave, the period of which depends on the angle between the beams. Through the photo-sensitive effect, that pattern is imprinted into the fiber as a periodically varying change in refractive index. Changing the period merely requires changing the angle of the mirrors.

Early demonstrations of FBG fabrication used such as interferometric approach, but the stability of the interference pattern could easily be compromised by mechanical vibrations. A more reliable method for volume manufacturing uses phase masks to contact print the gratins. A phase mask is itself a grating, etched in silica that diffracts.

UV light at normal incidence into the +1 and -1 diffractive orders. These two orders interfere to create the desired interference pattern just behind the mask, which is where the fiber is placed. Typical exposure times vary from a few seconds to a few minutes, depending on the type and strength of grating.

2.2 Photonic Crystal Fibers

A new class of optical fiber, called photonic crystal fiber (PCF) [8] has attracted considerable interest since their initial invention for their unusual optical properties. These fibers are characterized by microscopic air holes running along the fiber thorough the entire length of the fiber. These fibers are also known as microstructured fibers. Among the interesting novel features associated with these fibers are their endless single-mode operation from UV to IR spectral region, easy tolerance for dispersion and polarization control, possibility of obtaining large core single mode fiber and zero group velocity dispersion at short wavelength. These features mean that they are the subject of a growing research and development effort. The special index profile of microstructures fibers leads to exceptional guiding properties which cannot be obtained in the conventional step index fibers. The structure provides a wavelength dependent effective index for the cladding for which single mode guidance for a large range of wavelength

becomes possible. There is a class of PCF in which the arrangement of air holes need not be regular and periodic fashion. These fibers are also referred to as holey fibers.

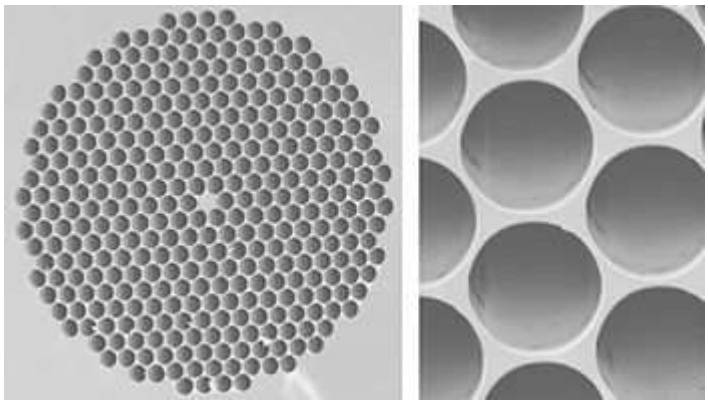

Figure 2.2: Photonic crystal fiber cross section

(Source- P. S. J. Russell, "Photonic crystal fibers", *Science*, vol.299, p.358 (2003).)

The light guidance through the microstructed fibers can take place by two different mechanisms: average effective refractive index index effect and photonic bandgap effect. For average refractive index model, the cladding full of air holes are replaced by a layer of average refractive index and the light guidance can be explained by simple and conventional principle of successive total internal reflection. For this model the array of air holes need not be regular, periodic, lattice-like structure. For the photonic bandgap mechanism of light guidance through a fiber, periodic arrangements of air holes are essential and these fibers are called photonic bandgap fibers. In these fibers the periodic arrangement of air holes in the cladding region of the fiber leads to the formation of photonic bandgap in the transverse plane of the fiber. Frequencies within this band gap cannot propagate in the cladding and are thus confined to propagate within the core which acts as a defect in the otherwise 'perfect' periodic structure.

In 1991, the idea emerged that light could be trapped inside a hollow fiber by creating a periodic wavelength-scale lattice of microscopic holes in the cladding glass known as a photonic crystal. To understand how this might work, consider that all wavelength-scale periodic structures exhibit ranges of angle and color ("stop bands") where incident light is strongly reflected. This is the origin of the color in butterfly wings, peacock feathers, and holograms such as those found on credit cards. In photonic band gap (PBG)

materials, however, these stop bands broaden to block propagation in every direction, resulting in the suppression of all optical vibrations within the range of wavelengths spanned by the photonic band gap. Appropriately designed, the holey photonic crystal cladding, running along the entire length of the fiber, can prevent the escape of light from a hollow core. Thus, it becomes possible to escape the strait jacket of total internal reflection and trap light in a hollow fiber core surrounded by glass.

In the early 1970s , there had been the suggestion that a cylindrical Bragg waveguide might be produced in which rings of high and low refractive index are arranged around a central core. Recently a successful solid-core version of this structure, made using modified chemical (MCVD), was reported. The effort is now heading toward a hollow core version, an ambitious goal that requires a materials system with much larger refractive index constrant than the few percent offered by MCVD [9].

There are various applications of it. Among the more important ones, are rare-earth doped lasers and amplifiers and sensors. Also, the possibility of fashioning fibers from traditionally " difficult " materials such as infrared glass opens up the prospect of a single- mode fiber that could transmit 10.6 µm light with low loss and at high powers; this would revolutionize the field of laser machining.

Photonic crystal fibers represent a next-generation, radically improved version of a well-established and highly successful technology. In escaping from the confines of conventional fiber optics, PCFs have created a renaissance of new possibilities in a large number of diverse areas of research and technology, in the process irrevocably breaking many of the tenets of received wisdom in fiber optics.

Through photonic band gap manipulation cladding material can be engineered that does not support any modes for certain frequencies, creating total internal reflection. The engineerable birefringence allows for relatively high refractive index contrasts. This allows a mode to be confined in a core much smaller than previously possible, less than the wavelength of the light. The current performance of single-mode optical fibers results from many years of intensive research. There appears to be no reason why the losses in Photonic Crystal Fibers cannot be reduced to or below that of standard optical fibers. Similar development effort could lead to explosive growth in photonic crystal fiber technology over the coming years.

2.3 Segmented Cladding Fibers

A new type of fiber, known as segmented cladding fiber (SCF) [10] were proposed as an alternative to the holey fibers for the provision of single mode operation over an extended range of wavelengths. It was then shown that an SCF could be designed as an ultra large core single mode fiber for optical communication, which could suppress effectively the non-linear optical effects because of its large core size. It also provides a much higher transmission capacity because of its potentially weak birefringence, compared with a holey fiber.

A SCF is characterized by the cladding with regions of high and low refractive index alternating regularly with uniform core of high refractiv index. The SCF uses small index contrast unlike holey fiber and hence exhibits some better qualities over photonic crystal fibers. It has potentially low polarization mode dispersion which is essential for high bit rate transmission. The chromatic dispersion of SCF is also expected to be similar to that of conventional fiber so that it can be controlled by conventional techniques. An SCF can be bare segmented cladding fiber or coated segmented cladding fiber. For the former, the segmented cladding is surrounding by air and for the latter, the segmented cladding of the SCF extends to infinity. The effective index decreases monotonously towards the core index and eventually exceeds the mode index of the fundamental mode. An infinitely extended SCF is therefore a leaky structure and all the modes of the fiber suffer from leakage loss. In practice, the fiber is truncated a finite cladding radius and coated with a high index material. A high index surrounding is similar to that of an infinitely extended cladding and at the same time shields the fiber from external perturbations.

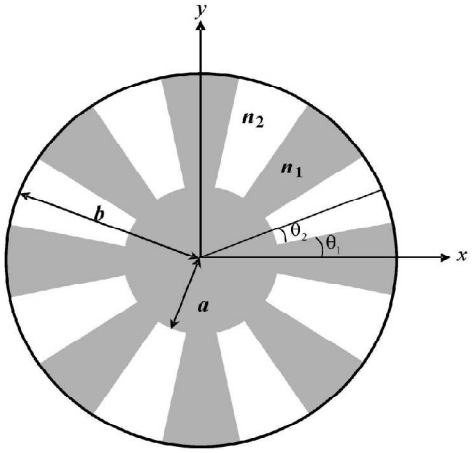

Fig 2.3 Transverse cross-section of the SCF.

(Source- V. Rastogi and K. S. Chiang, "Propagation characteristics of a segmented cladding fiber", Opt. Lett., vol.26, pp.491-496 (2001).)

2.4 Large Mode Area Fibers

Multimode optical fiber cannot be used for long distance data transmission due to the intermodal dispersion. Fiber non-linear effects limit the bit transfer rate for single mode fiber because of its small core diameter. In recent years, large-mode-area-fibers have attracted our considerable interest because increased mode field area allows higher peak power within the core before non-linear effects become significant and operative. Longer amplifier spacing can also be used for higher effective area.

Single mode fiber with low dispersion slope and large core area is most desirable for long-haul terrestrial and submarine transmission system and high capacity DWDM system. But, large mode area allows a number of modes to propagate. In the case of conventional fibers, the effective area is limited by the fact that an increasing core size requires a correspondingly decreasing index step between the core and the cladding in order to maintain single-mode operation. This imposes requirements on the control of the index profile which is difficult to realize with doping of the glass.

Knight et al. [11] showed that ultra large core single mode fiber can be achieved from a holey fiber by suitably choosing the hole diameter and spacing. They have fabricated a holey fiber with a core diameter of 22.5 μm, the number of guide mode of this fiber does not depend on core radius and wavelength.

Mortensen et al. [12] worked on the photonic crystal fiber and found that enhancement of mode area by 30% can be achieved without a corresponding decrease in attenuation. They demonstrated that triangular distribution of air hole in the cladding and suitable chose of hole diameter can improve the mode area and the loss properties of holey fiber.

To date, most work in this area has concentrated on rare-earth-doped optical fiber with large mode area to improve their energy storage characteristics in compromise of gain efficiency. A number of erbium doped fiber with large mode area have been fabricated which demonstrated their effectiveness as optical amplifiers and in Q-switched fiber lasers. Yin et. Al [13] made a new design of fiber having large effective area over 100 μm^2 which can be used in DWDM system for its non-zero dispersion shifting characteristics. This fiber also showed low bending and splicing loss.

2.5 Raised Inner Cladding Fibers

These fibers consist of five layers of which four layers form the cladding. The cladding layers have low and high indices alternatively.

The objective of this structure has low loss and low dispersion at both the 1.3 µm and 1.55 µm wavelengths. This fiber shows uniform dispersion properties in this wavelength range.

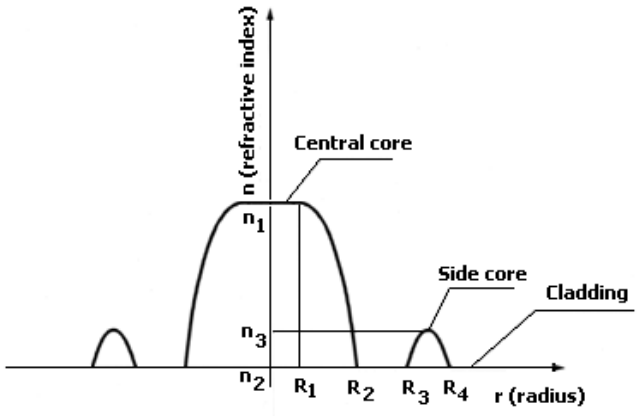

Figure 2.3: Refractive index profile of raised inner cladding fiber

(Source -L. G. Cohen, D. Marcus and W. L. Mammuel, “Radiating leaky mode losses in single mode lightguide and depressed index claddings”, IEEE trans. J. Quant. Electron., vol.18, pp. 1467-1471 (1982).)

2.6 Large Mode Area Multiclad Leaky Fiber

LMA multiclad leaky fibers are used in effective single mode operation by large differential leakage loss between the fundamental mode and the higher order modes [14,15,16]. These designs include periodically arranged high and low refractive index segments in the angular direction of cladding a graded index cladding with radially rising refractive index [17] and a cladding mode of periodically arranged low index trenches of varying strength in an otherwise high index medium [18].

2.7 Depressed Inner Cladding (DIC) Fibers

These fibers have two claddings and are also called double clad fibers. Each cladding has a refractive index that is lower than that of the core. Of the two claddings, inner and outer , the inner cladding has the lower refractive index. A doubly clad fiber has the advantage of very low macrobending losses. It also has two zero-dispersion points and low dispersion over a much wider wavelength range than a singly clad fiber [19].

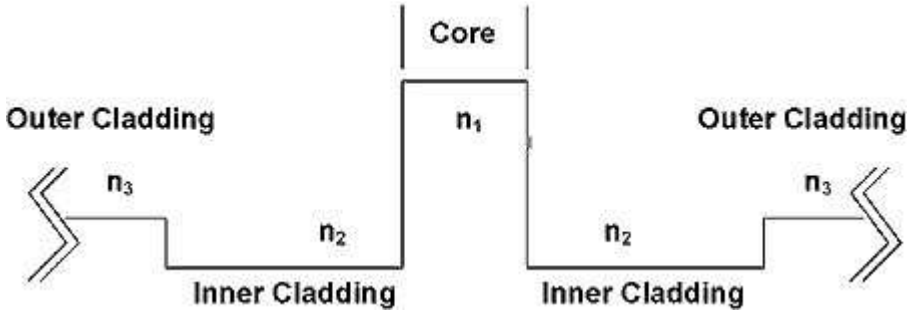

Fig 2.4 Refractive index profile of typical DIC fiber

2.8 EXAMPLES OF INTEGRATED WAVEGUIDES

Refractive indices of materials employed to build optical waveguides

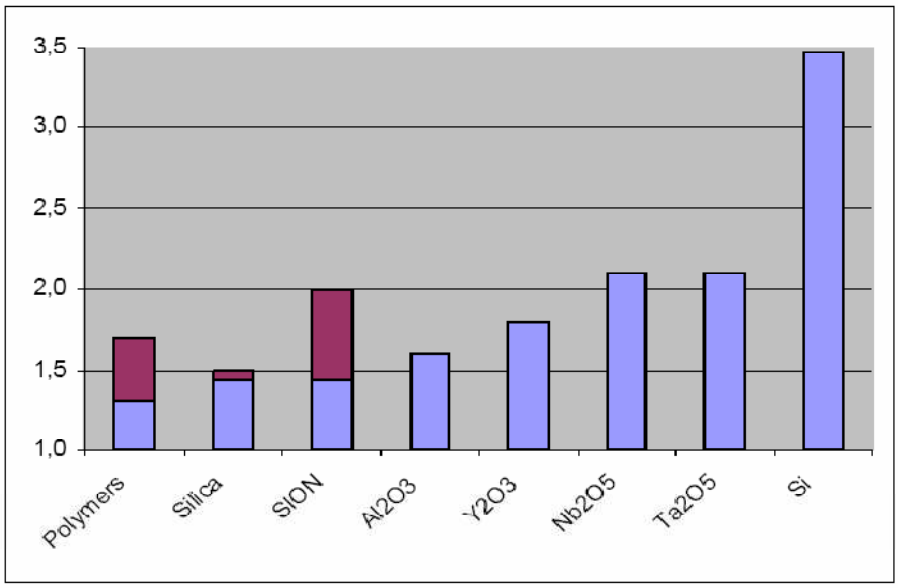

Fig.2.5 Plot showing refractive index of various materials used in optical waveguides

(Source- Fundamentals of Integrated Optical Waveguides:Alejandro Martinez)

Silica (SiO_2) Waveguides:

Core: doped silica; claddings: silica (n=1.45)

Advantages:mature technology, ultra-low propagation losses, low fiber coupling losses, tuning by thermal effects.

Drawbacks:large bending radius (large size devices), weak nonlinearities, no integration with active devices .

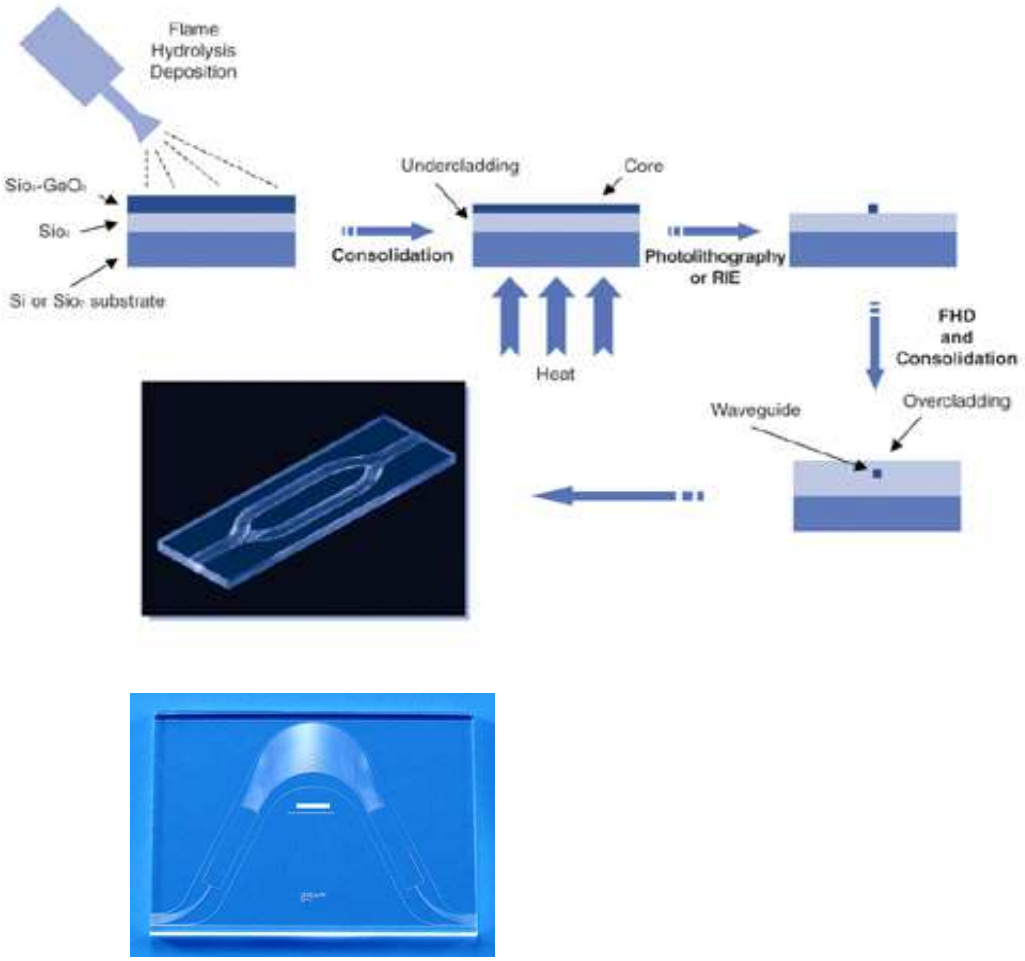

Fig.2.6 Fabrication of optical waveguide using silica as material

Polymer Waveguides

Core: polymer; claddings: air, lower index polymer, silica

Similar to the case of the silica waveguides.

Advantage: Some polymers can be designed to have very high nonlinearities-highly suitable for nonlinear applications.

The index can be varied over a wider range.

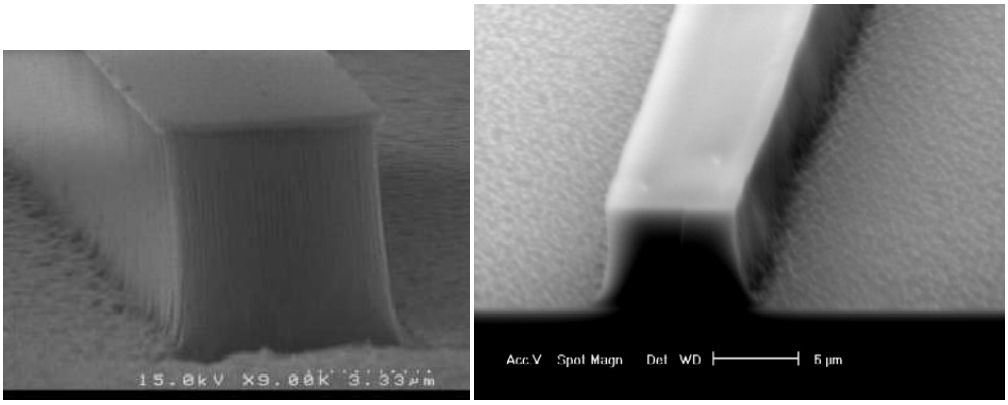

Fig.2.7 Cross –sectional view of Polymer waveguide

(Source- Fundamentals of Integrated Optical Waveguides:Alejandro Martinez)

Lithium niobate ($LiNbO_3$**) Waveguides**

Core: diffused Titanium in $LiNbO_3$*; claddings:* $LiNbO_3$*, air*

Advantages: mature technology, high electro-optic effect (electro-optical Mach-Zehnder modulators), efficient coupling to fibre.

Drawbacks: low integration density, polarization dependence, no mass-manufacturing $LiNbO_3$.

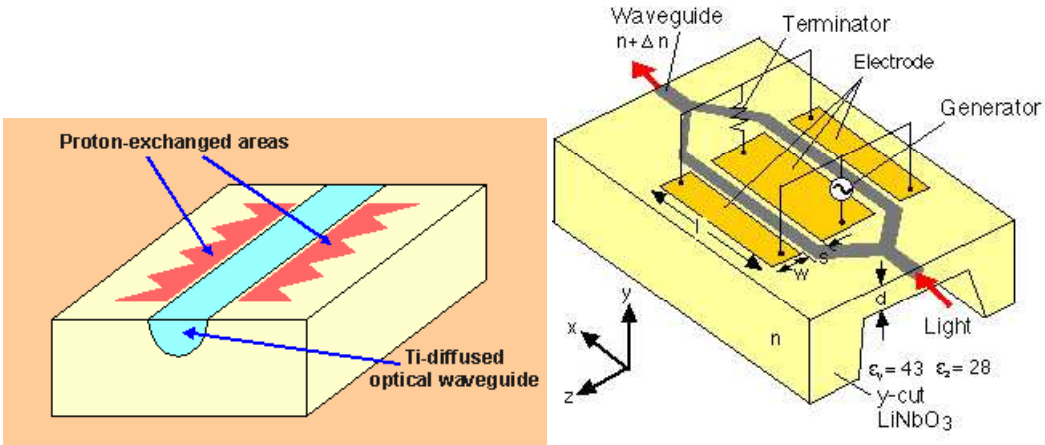

Fig.2.8 Structure of Lithium-niobate waveguide

(Source- Fundamentals of Integrated Optical Waveguides:Alejandro Martinez)

Silicon Wires (Strip Waveguides)

Core: Silicon (n=3.5); claddings: silica, air

Advantages: Integration of on-chip electronics/photonics, mass manufacturing, high density of integration, strong confinement.

Drawbacks: propagation losses (>1dB/cm), weak nonlinearities, negligible electro-optic effect, inefficient coupling.

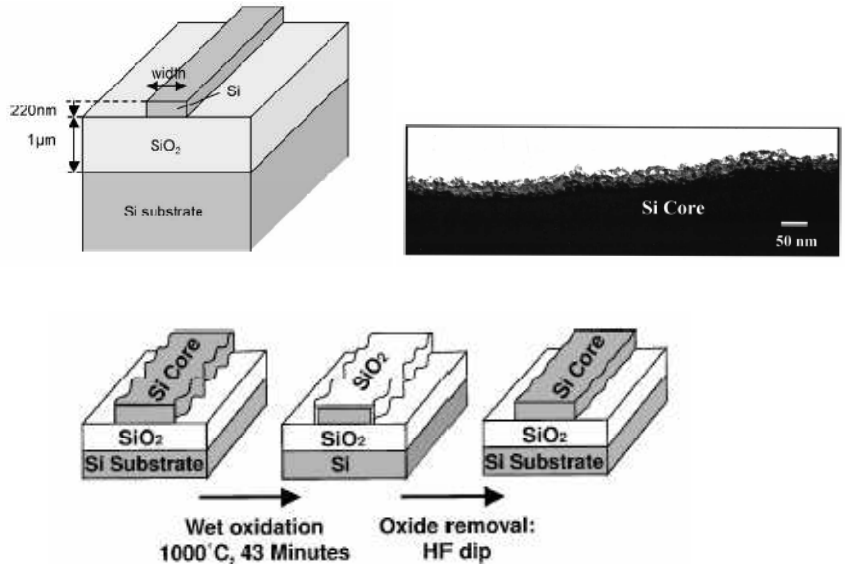

Fig.2.9 Fabrication of strip waveguide

(Source- Fundamentals of Integrated Optical Waveguides:Alejandro Martinez)

III-V (GaAs, InP) Waveguides

Core: n≅3.5; claddings: slightly lower than the core index

Advantages: high nonlinearities (switching functionalities), integration with lasers and detectors, low losses, high efficient coupling to fiber.

Drawbacks: not suitable for mass manufacturing GaAs rib waveguide .

III-V heterostructures

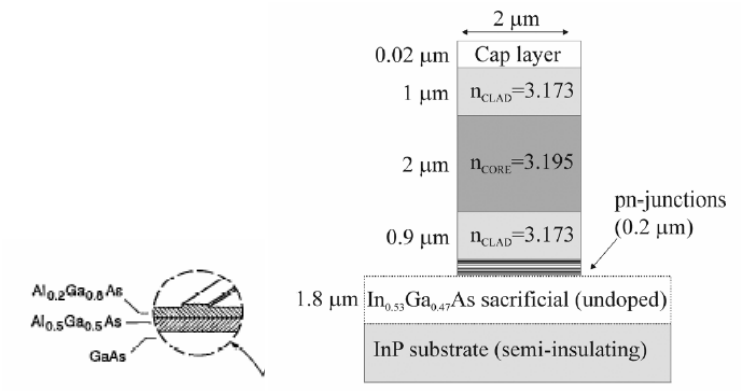

AlGaAs/GaAs heterostructure

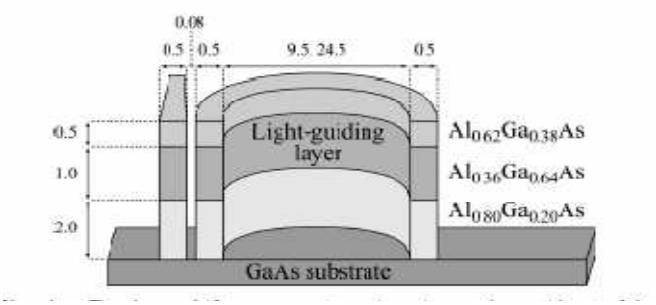

Fig.2.10. Heterostructure waveguide

(Source- Fundamentals of Integrated Optical Waveguides:Alejandro Martinez)

Chapter 3

Leaky channel waveguide for high-power applications

Aim of this thesis is to present a leaky channel waveguide for high-power applications. A suitable waveguide design for high-power laser is one which can support only single-mode for propagation even with a suitably large mode area [20]. The proposed waveguide works on the principle of **mode filtering**. Waveguide has been analyzed by EIM and TMM to calculate the leakage losses of the modes.

3.1 Proposed design

The waveguide structure is characterized by a rectangular core and a geometrically shaped cladding, which is so designed that all the modes are leaky. The refractive index profile of the proposed design is shown in the fig.3.1 and is defined as

$$n(\mathrm{r}) = \begin{cases} n1\,; & 0 < y < a \\ n2\,; & a < y < b \\ n1\,; & b < y < c \\ n3\,; & c < y < d \\ n1\,; & d < y < e \\ n4\,; & e < y < f \\ n1\,; & y > f \end{cases} \qquad (3.1)$$

where $n_1 > n_4 > n_3 > n_2$

The high index regions 0 < y < a, b < y < c and d < y < e define inner and outer cores of the fiber, respectively. The regions a < y < b, c < y < d and e < y < f are depressed cladding regions and can be defined as inner and outer cladding. Outermost high index region (y > f) makes the overall design leaky, and all the modes suffer from finite leakage loss. The width of different layers are defined as $d_1 = b - a$, $d_{high} = c - b$, $d_2 = d - c$, $d_{high} = e - d$ and $d_3 = f - e$.

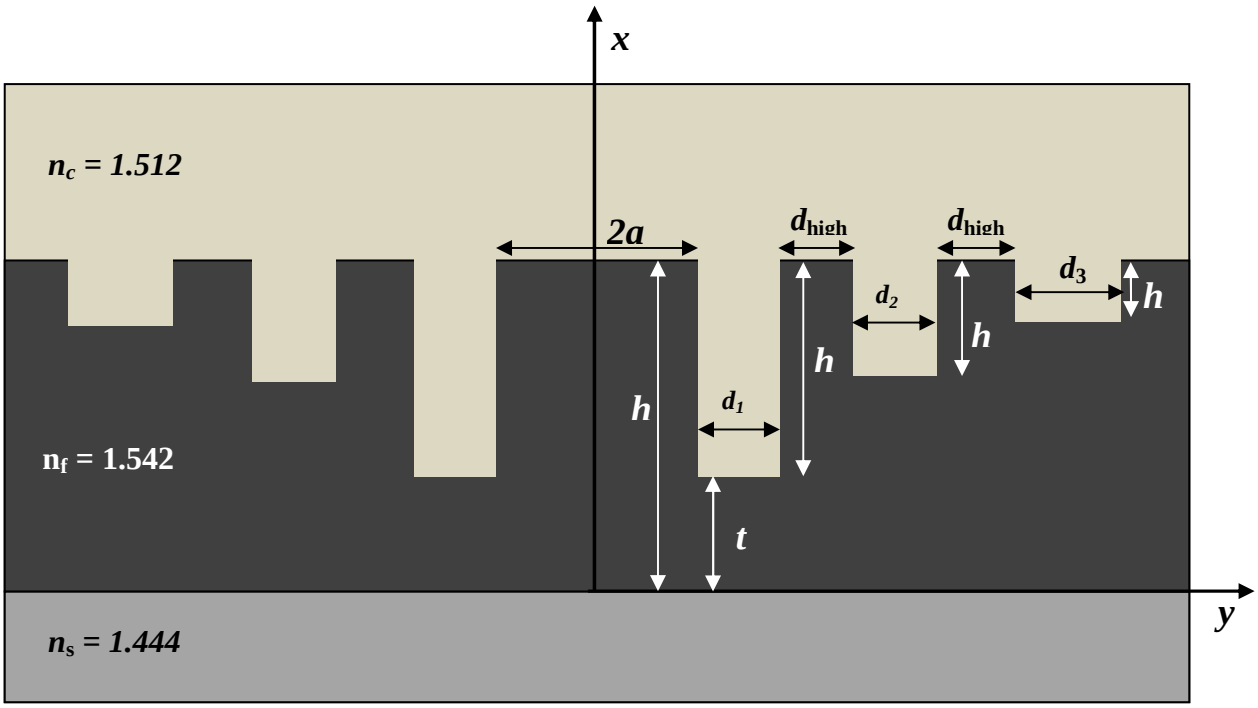

Figure 3.1: Proposed Leaky structure

Proposed design with suitable design parameters ensure effective single-mode operation by introducing high leakage loss to higher-order modes while a nominal loss to the fundamental mode. Overall design is leaky and supports a finite leakage loss to all the modes of waveguide. Leaky cladding consists of three trenches of variable depth and thickness. Depth of the trench decreases as one move away from the rectangular core. Performance of the waveguide depends upon the leakage losses of the first two modes. We have analyzed the waveguide by using effective- index method (EIM) in conjunction with the transfer-matrix-method (TMM) by calculating the effective indices and the leakage losses of the modes. Proposed waveguide can be fabricated in polymer geometry by reactive-ion etching technique and is expected to find applications in designing high-power lasers.

3.2 Effective Index Method

EIM is a well established method for solving rectangular-core waveguides. This method is particularly accurate for large-core structure that is operated at a large normalized

frequency. The idea of the method is to convert approximately a two- dimensional waveguide into an equivalent one-dimensional waveguide with an effective refractive-index profile that depends upon the geometry of the waveguide. Thus, the method requires only the solutions of planar waveguides. There are two ways of applying the method to solve the same waveguide: the x-method and the y-method. We use the y-method in which the waveguide structure is first solved in the x-direction for the TM_{n-1} (TE_{n-1}) mode to obtain a y-dependent effective-index profile, which is then solved by the TMM for the TE_{m-1} (TM_{m-1}) mode to get the propagation constant for the E_{mn}^{x} (E_{mn}^{y}) mode, where the superscripts x and y denote the polarization of the mode and m (= 1,2,3, …) and n (= 1,2,3, …) are the mode orders. Then the TMM is used to divide the effective-index profile into many uniform layers, each of which is represented by a 2 × 2 matrix that relates the field coefficients for that layer. By applying boundary conditions at the interfaces of different layers, a matrix equation is obtained from which the propagation constants of the modes can be found with a root-searching algorithm.

3.3 Transfer Matrix Method

There has been considerable interest in developing accurate numerical approximate techniques to study the propagation characteristics of absorbing, non-absorbing or leaky planar waveguide structures. The use of the matrix method in studying the propagation of plane electromagnetic waves through a stratified medium is well known in optics. Since a planar waveguide is nothing more than a stack of thin films, the standard mathematical methods used in the analysis of optical coatings, such as interference filters can be extended to include optical waveguides. In essence this method involves determination of the transfer matrix of the system and then using the properties of a guided mode to obtain a characteristic equation. The solutions of this transcendental equation give the propagation constants of the modes of the waveguide. We have first obtained the effective-index profile of the proposed design by using effective index method. Then the TMM [21] is used to divide the effective-index profile into many uniform layers, each of which is represented by a 2 × 2 matrix that relates the field coefficients for that layer. By applying boundary conditions at the interfaces of different layers, a matrix equation is obtained from which the propagation constants of the modes can be found with a root-searching algorithm. In our case, the refractive index of the outermost layer is equal to the core index, which makes structure leaky and hence all

the supported modes suffer from finite leakage loss. The boundary condition for an outgoing wave in the outermost layer leads to a matrix equation that admits complex propagation constants. The real part of the propagation constant gives the effective index of the mode, which determines the dispersion characteristics of the structure, while the imaginary part gives the leakage loss of the mode, which plays an important role in determining the single-mode operation of the structure. For the determination of the single-mode condition, we have compared the leakage losses of first two modes only because, in general the leakage loss increases with the mode order.

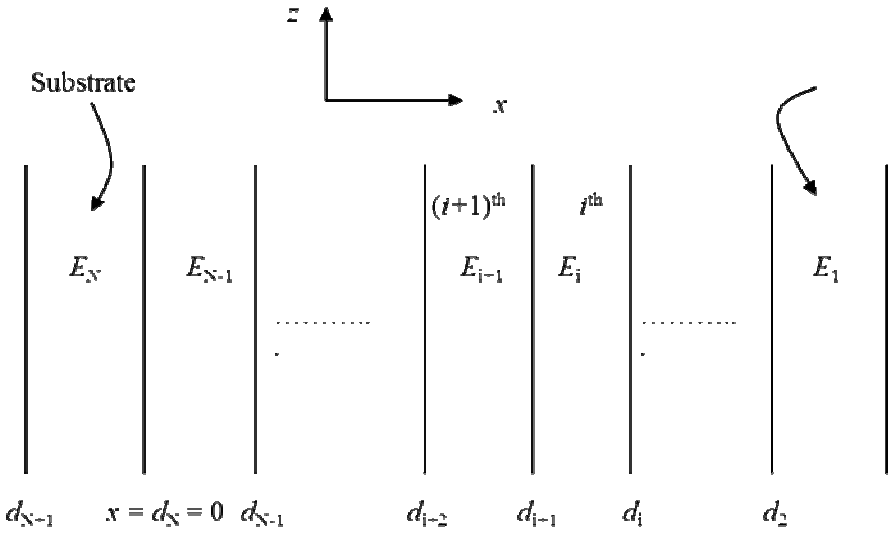

Figure 3.2: Stair case representation of the channel leaky waveguide

To implement the TMM, the refractive-index profile of the structure is first divided into a large number of homogeneous layers as shown in Fig. The electric field in the ith layer with refractive index n_i can be written as

$$E_i = \begin{cases} C_i \cos[k_i(x-d_{i+1})] + D_i \sin[k_i(x-d_{i+1})] & \kappa_i^2 > 0 \\ C_i \cosh[k_i(x-d_{i+1})] + D_i \sinh[k_i(x-d_{i+1})] & \kappa_i^2 < 0 \end{cases} \quad (3.2)$$

where $k_i = |\kappa_i|$, $\kappa_i^2 = k_0^2 (n_i^2 - n_{\text{eff}}^2)$, $k_0 = 2\pi/\lambda$ is the free-space wavenumber, and n_{eff} = = β/k0 is the effective index of the mode with β being the propagation constant. By applying suitable boundary conditions at the interface between the i^{th} and $(i+1)^{\text{th}}$ layers, the field coefficients, , C_i, D_i, C_{i+1}, and D_{i+1}, are related by a 2×2 matrix:

$$\begin{pmatrix} C_{i+1} \\ D_{i+1} \end{pmatrix} = S_i \begin{pmatrix} C_i \\ D_i \end{pmatrix} \tag{3.3}$$

where Si is known as the transfer matrix of the ith layer. For the TE mode, Si is given by for

$$S_i = \begin{pmatrix} \cos\Delta_{i+1} & -\left(\frac{k_i}{k_{i+1}}\right)\sin\Delta_{i+1} \\ \sin\Delta_{i+1} & \left(\frac{k_i}{k_{i+1}}\right)\cos\Delta_{i+1} \end{pmatrix} \quad \text{for } \kappa_i^2 > 0 \tag{3.4}$$

$$\begin{pmatrix} \cosh\Delta_{i+1} & \left(\frac{k_i}{k_{i+1}}\right)\sinh\Delta_{i+1} \\ \sinh\Delta_{i+1} & \left(\frac{k_i}{k_{i+1}}\right)\cosh\Delta_{i+1} \end{pmatrix} \quad \text{for } \kappa_i^2 < 0$$

where $\Delta_i = k_i(d_i - d_{i+1})$. The field coefficients of the last layer can be related to the field coefficients of the first layer by simply multiplying the transfer matrices of all layers:

$$\begin{pmatrix} C_N \\ D_N \end{pmatrix} = f \begin{pmatrix} C_1 \\ D_1 \end{pmatrix} \tag{3.5}$$

where $f = S_{N-1}S_{N-2}.....S_1$ with

$$f = \begin{pmatrix} f_{11} & f_{12} \\ f_{21} & f_{22} \end{pmatrix} \tag{3.6}$$

In the high-index outermost layer only the outgoing wave exists and in the low-index substrate region no amplification is allowed. These conditions give $C_1 = iD_1$ and $C_N = -D_N$. From Eqs. (5) and (6), we can write

$$C_N = (f_{12} + if_{11})\, D_1 \quad \text{and} \quad D_N = (f_{22} + if_{21})\, D_1 \tag{3.7}$$

Equating C_N and $-D_N$ from Eq. (7), we obtain an eigenvalue equation for the propagation constant β, i.e., $F(\beta) = 0$. In general, the propagation constant can be expressed as $\beta = \beta_r + i\beta_i$ with β_r being the real part and β_i the imaginary part. A plot of $1/|F|^2$ with β shows a number of resonance peaks, each of which corresponds to a mode. These peaks are Lorentzian in shape. The value of β corresponding to the resonance peak gives the real part of the propagation constant β_r and the FWHM of the Lorentzian gives the imaginary part β_i. In this way, both the real part and the imaginary part of β can be calculated.

Chapter 4

Result and Discussions

For the proposed leaky waveguide structure, following results are obtained which are responsible for large mode area single mode operation used in designing high-power lasers and amplifiers. This section has been divided into 7 subsections to discuss all the features of the proposed structures. In subsection (4.1), we have discussed the effect of changing the trench's width namely d_1 and d_2 on the leakage losses of fundamental and the first higher order modes present. In the next subsection (4.2), we discuss the effect of changing core width '*a*' on the leakage loss of modes. The effect of parameter '*t*' on the leakage loss of fundamental and first higher mode is demonstrated in subsection (4.3). In the subsection (4.4), an example of an all solid design with a large core area for extended single-mode operation over the range of wavelengths (900 - 1600 nm) is shown. In the subsection (4.5), we presented the effective index profile of the proposed design at 1550 and 900 nm. The spectral variation of mode area is shown in section (4.6).

We have carried out numerical calculations for the following parameters:

n_f = 1.542, n_s = 1.444, n_c =1.512, a = 5 μm

d_1 = 4 μm, d_2 = 3 μm, d_3 = 5 μm and d_{high}= 3μm

h =10 μm, h_1 = 6 μm, h_2 = 4 μm and h_3 = 2 μm and λ= 1.55μm

4.1 Effect Of The Cladding Parameters

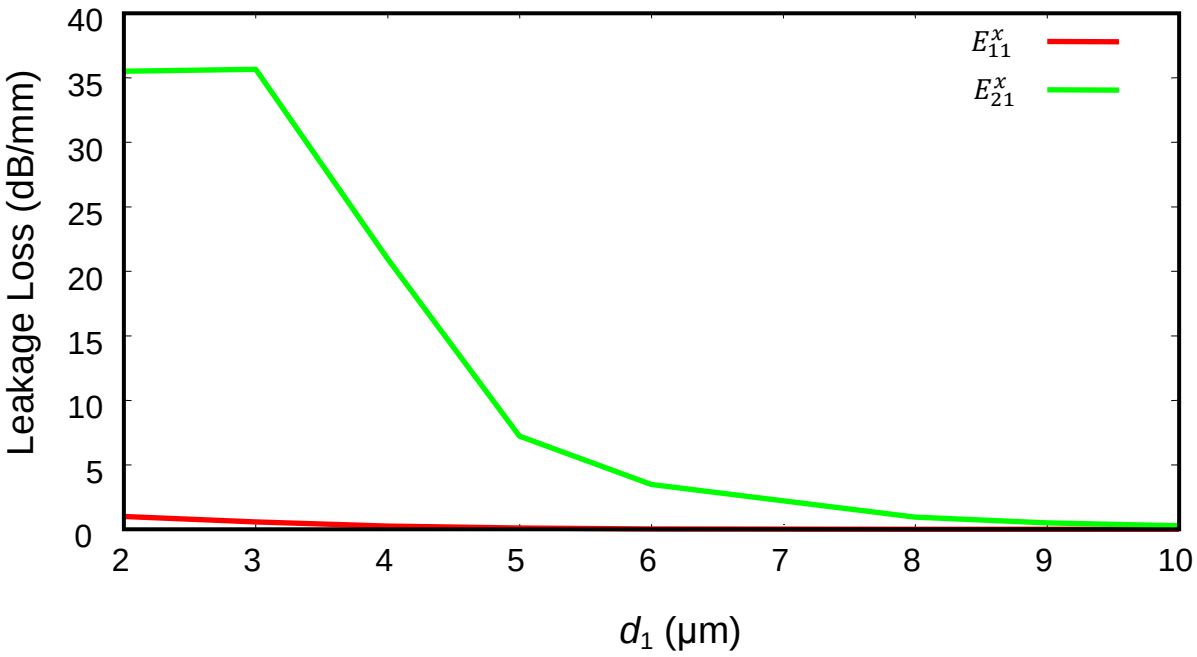

Figure 4.1: Variation of leakage loss of E_{11}^x *and* E_{21}^x with d_1

The leakage loss of a particular mode depends on the distance from the core at which the effective refractive index of the cladding becomes equal to the effective index of the mode. The larger this distance is, the smaller is the leakage loss. The differential leakage loss depends on the relative leaking distances of the two modes. It is seen that the leakage loss decreases with an increase in the value of trench width d_1 , which is the result of moving the leaky cladding away from the core. So, the loss experienced by the fundamental mode i.e. E_{11}^{x} is less compared to that of higher order mode $\mathrm{E}_{21}^{\mathrm{x}}$. The leakage loss of E_{11}^{x} and E_{21}^{x} mode starts at 2 dB/mm and 36 dB/mm respectively.

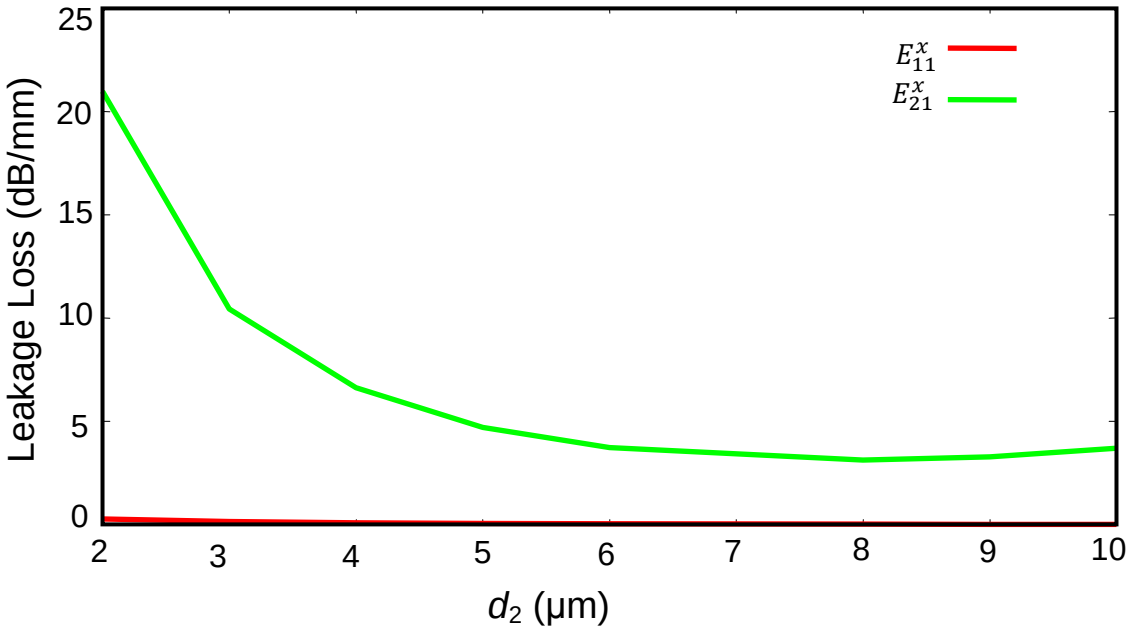

Figure 4.2: Variation of leakage loss of E_{11}^x *and* E_{21}^x with d_2

It is clear from the above plot that the leakage loss suffered by both the fundamental mode E_{11}^x and the first higher order mode E_{21}^x is less than in previous case (leakage loss of E_{21}^x starts at 21 dB/mm and E_{11}^x at 0.5 dB/mm) as the leaky cladding region now shifts farther away the central core region. So, there is a decrease in resonant coupling of modes.

4.2 Effect Of Changing Core Width '*a*'

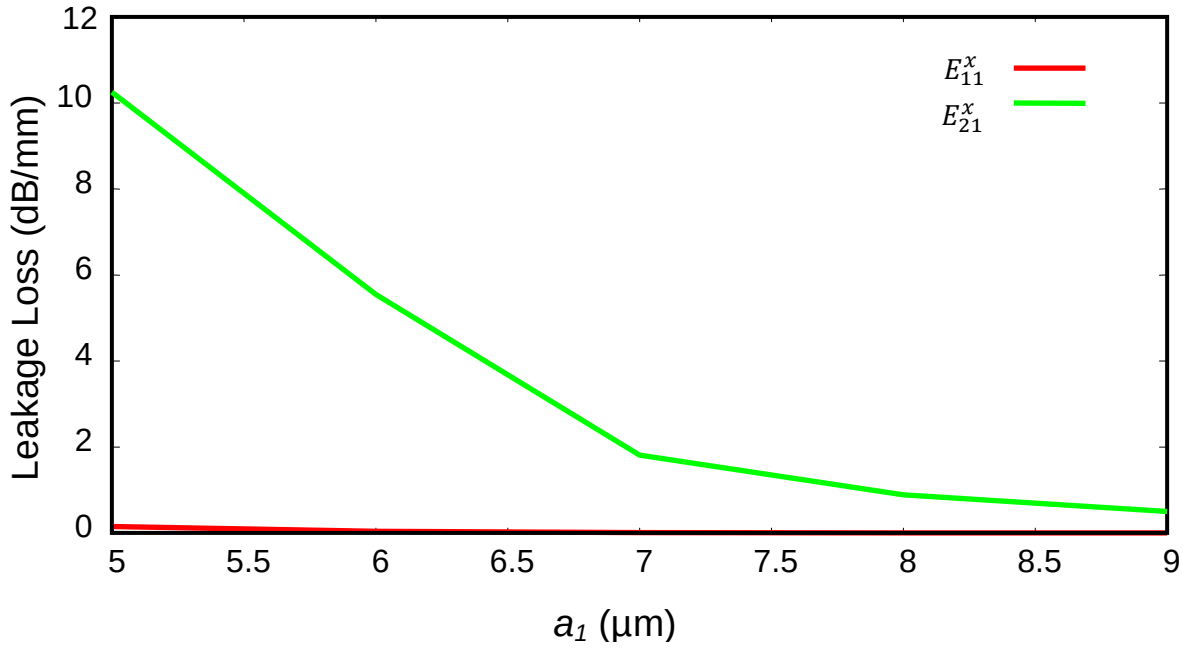

Figure 4.3 : Variation of leakage loss of E_{11}^x *and* E_{21}^x with a_1

Figure 4.3 shows the effect of the core width *a* on the leakage loss for *h* = 10 μm and λ = 1550 nm. An increase in the core width leads to a tighter light confinement in the core and hence a lower leakage loss (using the equation $V = (2\pi/\lambda)a\sqrt{(n_2^2 - n_1^2)}$).However, the trend reverses when the value of *a* passes an optimum value beyond which the loss starts to rise because of the effects due to closing the gap between the leaky cladding and the core.

4.3 Effect Of The Parameter '*t* '

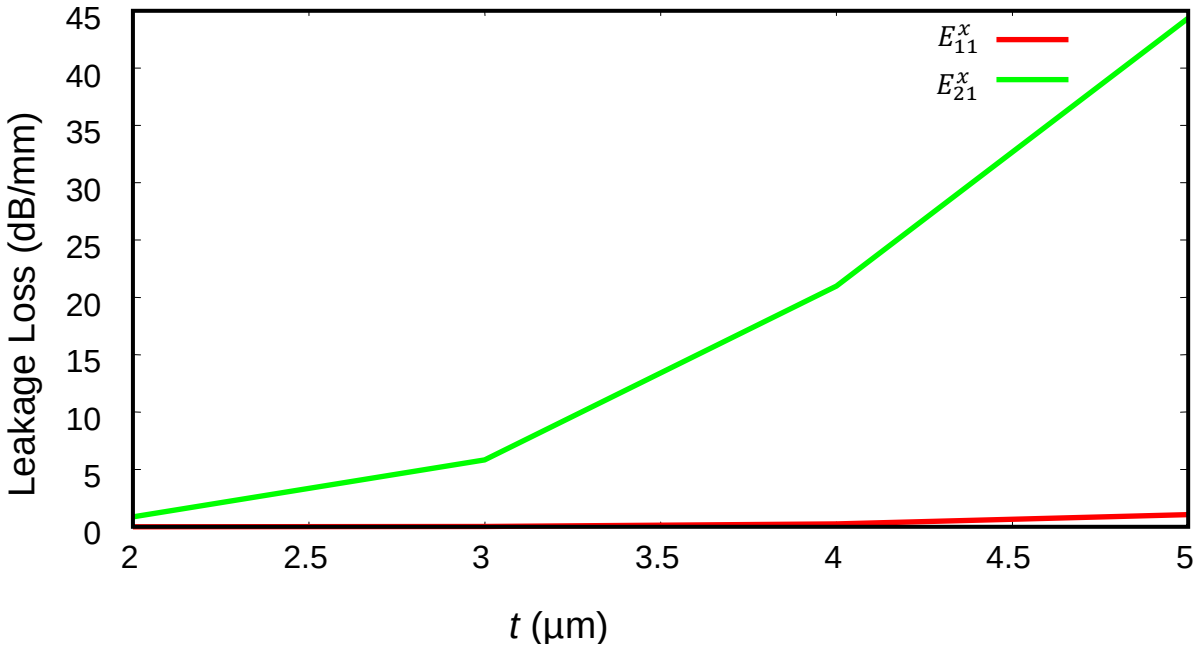

Figure 4.4: Variation of leakage loss of E_{11}^x *and* E_{21}^x with '*t*'

The effects of the parameter '*t*' on the leakage losses at 1550 nm wavelength have been plotted in Fig.4.4. An increase in the value of '*t*' effectively decreases the core – cladding index contrast and, thus, increases the losses of the modes.

4.4 Extended Single-Mode Operation

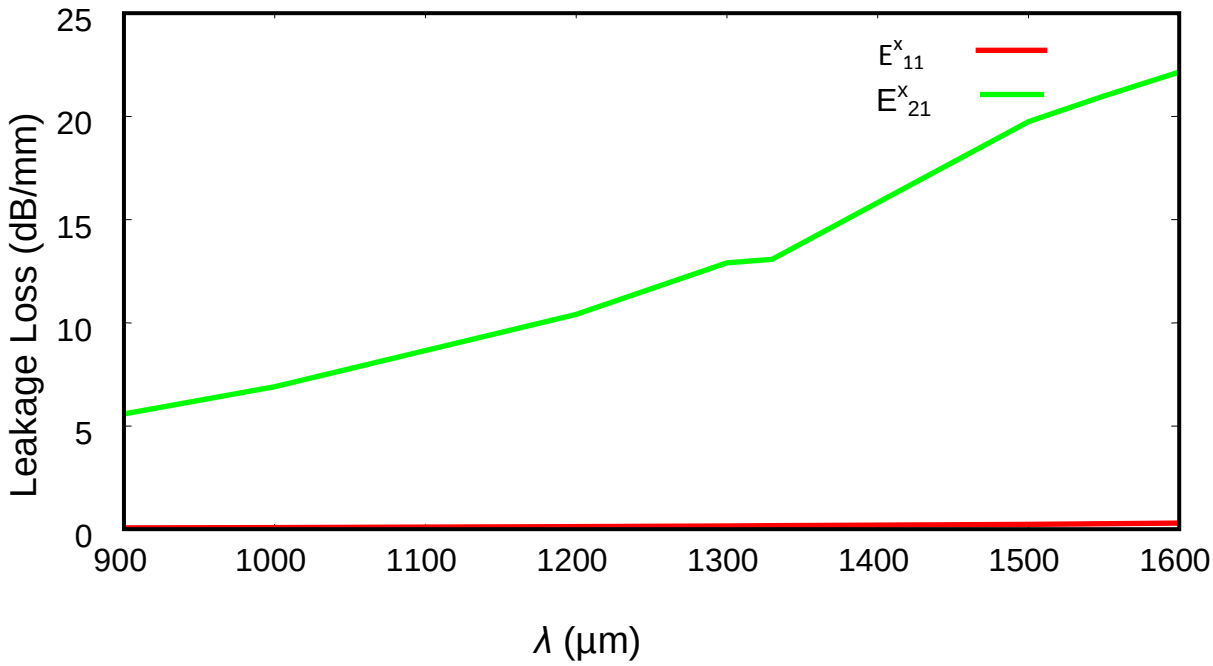

Figure 4.5: Variation of loss of E_{11}^{x} and E_{21}^{x} with change in wavelength

It is seen from above Fig. that the effective cladding profile is highly dispersive, which offers the possibility for extended single-mode operation. As an example, for a = 5 μm, h = 10 μm, t = 4 μm, the waveguide can exhibit extended single-mode operation. The figure shows the variations in the leakage losses of the first two modes in the wavelength range 900–1600 nm. In the entire wavelength range, the leakage loss of the E_{21}^{x} mode is higher than that of the fundamental mode by more than an order of magnitude. The maximum loss of the fundamental mode in this wavelength range is only 0.40 dB/mm (at 1600 nm), while the minimum loss of the E_{21}^{x} mode is 5.90 dB/mm (at 900 nm). The core area of this particular waveguide is 60μm^2. At 1550 nm, the leakage losses of the fundamental mode and the higher-order modes are 0.37 dB/mm and 18.66 dB/mm, respectively. So, waveguide of suitable length is sufficient to strip off all the higher-order modes at this wavelength.

4.5 Effective-Index Profiles at λ = 1550 nm and 900 nm

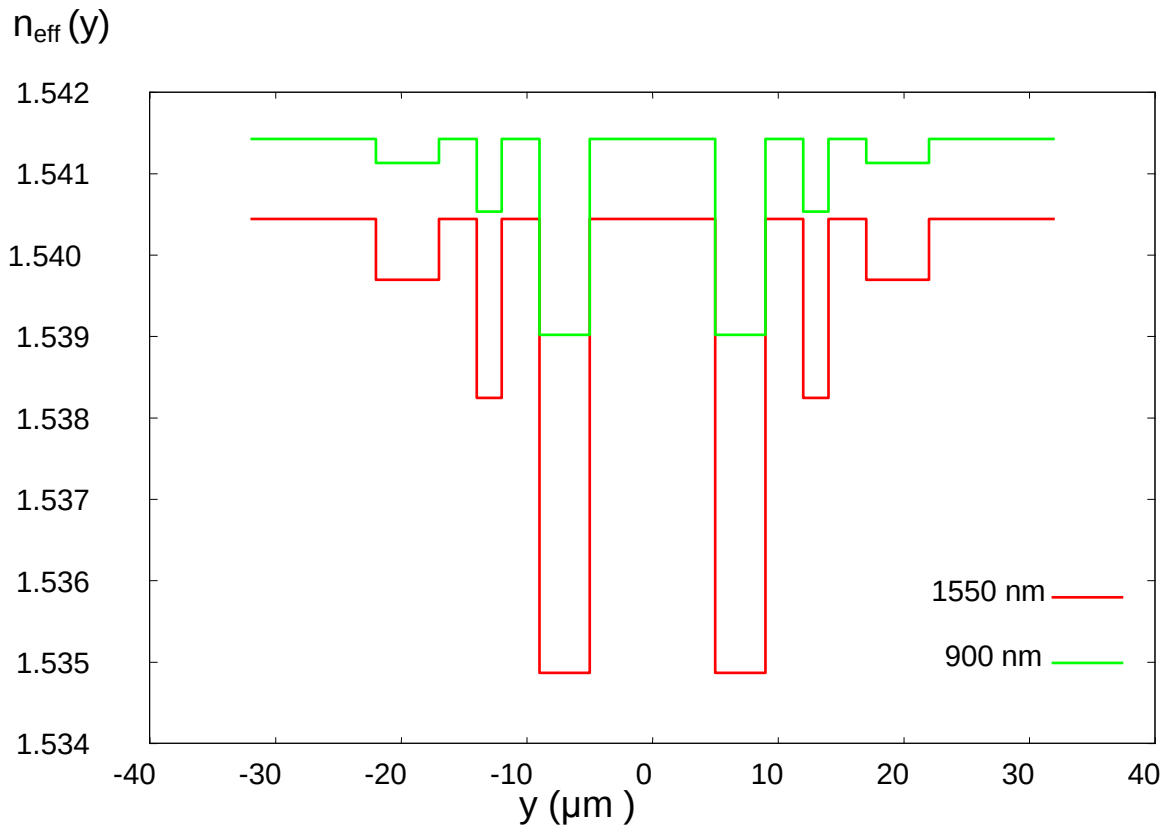

Figure 4.6: One-dimensional effective refractive-index profile obtained by the effective-index method at 1550 nm and 900 nm.

Figure 4.6 shows the effective-index profiles $n_{eff}(y)$ calculated for two different wavelengths λ = 1550 nm and λ =900 nm. The effective-index profile resembles the leaky step-index slab waveguide . As shown in Fig., the index of the cladding increases monotonically in the *y*-direction and eventually reaches the same value of the core index. In such a structure, the effective index of each mode is lower than the cladding index at a certain distance from the core and thus becomes leaky. If the leakage losses of all high-order modes are significantly larger than that of the fundamental mode, the structure operates effectively as a single-mode waveguide. In this way, the core can be made large to support effectively only the fundamental mode. The effective indices and

the leakage losses of the modes of the channel waveguide are calculated by solving the one-dimensional effective-index profile with the transfer matrix method.

4.6 Spectral Variation Of Mode Area Wth Wavelength

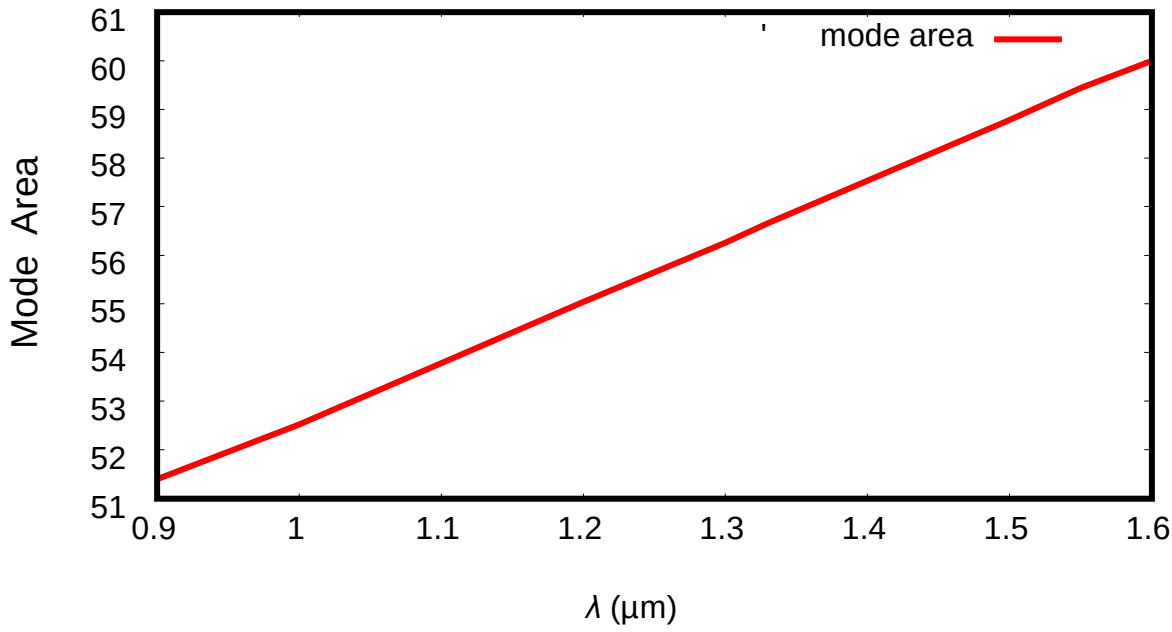

Figure 4.7: Spectral variation of mode area.

The effective mode area can be calculated using

$$A_{eff} = \frac{(\iint E^2 dx\, dy)^2}{\iint E^4 dx\, dy}$$

Where E is the amplitude of the Transverse Electric field propagating inside the waveguide.

The variation of mode area with wavelength is tabulated below-

λ (μm)	Mode area (μm^2)
0.900	51.4
1.00	52.6
1.20	55.3
1.30	56.6
1.33	57.03
1.50	59.3
1.55	60
1.60	60.6

It can be noted from the table that the mode area increases with increase in wavelength. Using the equation $V = (2\pi/\lambda)a\sqrt{(n_2^2 - n_1^2)}$, normalized frequency is inversely proportional to wavelength.So, as the value of wavelength increases, wave becomes less confined into the core region.Some part of core region spreads into the cladding region, resulting in increase in mode area.

Chapter 5

Conclusion and Scope for Future Work

A multi-layer channel waveguide is proposed that supports a single-guided mode with large-mode area. Geometrically shaped waveguide with suitable design parameters ensure effective single-mode operation by introducing high leakage loss to higher-order modes while a nominal loss to the fundamental mode. This is a great advantage. Typical design parameters shows that such a waveguide can provide single-mode operation with a core area as large as 100 μm^2 over an extended range of wavelengths (900–1600 nm), which can effectively suppress nonlinear optical effects and increase the power-handling capacity of the waveguide. Proposed waveguide can be fabricated in polymer geometry by reactive-ion etching technique. This class of waveguide is expected to find applications in high-power waveguide lasers and amplifiers.

The LMA design presented in this thesis can be extended to active materials to access the actual device performance. Moreover, Dispersion of the resonant design can also be studied for dispersion compensation applications.Various design parameters such as trench width , height and parameter ‘t’ can be tuned to obtain new LMA design with even better integrated optics applications.

REFERENCES

1. A. Ghatak and K. Thyagrajan, “Optical Electronics”.
2. Katsunari Okamoto, ‘‘Fundamentals of Optical Waveguides’'.
3. John Crisp, ‘‘Introduction to Fiber Optics’’.
4. Alejandro Martinez, ‘‘Fundamentals of Integrated Optical Waveguides’’.
5. H. J. Patrick, A. D. Kersey and F. Bucholtz, “Analysis of the response of long period fiber gratings to external index of refraction”, J Lightwave Technol. vol.16, pp. 1606-1612 (1998).
6. J. P. Meunier, J. Pigeon and J. N. Massot, “A numerical technique for determination of propagation characteristics of inhomogeneous planar optical waveguide”, Opt. Quantum Electron**.,** vol.15, pp. 77-79 (1983).
7. W. Liang, Y. Huang, Y. Xu, R. K. Lee, and A. Yariv, “Highly sensitive fiber bragg grating refractive index sensors”, Appl. Phys. Lett, vol.86, pp. 122-126 (2005).
8. P. S. J. Russell, “Photonic crystal fibers”, *Science*, vol.299, p.358 (2003).
9. D. H. Smithgall, T. J. Miller and R. E. Frazee, “A novel MCVD process control technique**”,** IEEE J. Lightwave Tech., vol. 4, pp.1360-1362 (1986).
10. V. Rastogi and K. S. Chiang, “Propagation characteristics of a segmented cladding fiber”, Opt. Lett., vol.26, pp.491-496 (2001).
11. J. C. Knight, T. A. Birks, R. F. Cregan, P. St. J. Russell and J. P. De Sandro, “Large mode area photonic crystal fibres”, Electron. Lett., vol.34, pp.134-141 (1998).
12. N. A. Mortensen, M. D. Nielsen, J. R. Folkenberg, A. Peterson and H. R. Simonsen, “Improved large mode area endlessly single mode photonic crystal fibers”, Opt. Express., vol.11, pp.456-460 (2002).
13. Y. Shizhuo, K. W. Chung, H. Liu, P. Kurtz and K. Reichard, “A new design for non-zero dispersion shifted fiber with a large effective area over 100 μm^2 and low bending and splicing loss”, Opt. Comm., vol.177, pp.225-229 (2000).
14. P. St. J. Russell, “Photonic crystal fibers”, Science, vol.299, pp. 358-360 (2003).
15. S. Sandgren, H. Ahlfeldt, B. Sahlgren, R. Stubbe, and G. Edwall “Fiber optical Bragg grating refractometer”, Fiber Integr. Opt., vol.17, pp. 51–62 (1998).

16. A. Kumar, V. Rastogi, C. Kakkar and B. Dussardier, “Co-axial duel-core leaky fiber for optical amplifiers”, Appl. Opt. vol.10, pp. 1464-1470 (2008).
17. K. Thyagarajan, S. Diggavi, A.Taneja, and A. K. Ghatak, “Simple numerical technique for the analysis of cylindrically symmetric refractive-index profile optical fibers”, Appl. Opt., vol.30, pp. 3877-3880 (1991).
18. A. Kumar, V. Rastogi and K. S. Chiang, “Leaky optical waveguide for high - power applications,” Applied Physics B, vol. 85, pp. 11-16, (2006).
19. A. Kumar, V. Rastogi and K. S. Chiang, “Large-core single-mode channel waveguide based on geometrically shaped leaky cladding,’’ Appl. Phys. B, vol. 90, 507–512 (2008).
20. A. Kumar, V. Rastogi, “Multi-layer cladding leaky planar waveguide for high-power applications’’, Appl Phys B, vol. 92, 577–583 (2008).
21. N. G. R. Broderick, H. L. Offerhause, D. J. Richardson, R. A. Sammut, J. Caplen and L. Dong, “Large mode area fibers for high power applications,” Opt. Fiber Technol., vol. 5, pp. 185-196, (1999).
22. J. Sakai and T. Kimura, “Large-core, broadband optical fiber,” Opt. Lett., vol. 1, pp. 169-171, (1977).
23. W. Wadsworth, R. Percival, G. Bouwmans, J. Knight, and P. Russell, “High power air-clad photonic crystal fibre laser,” Opt. Exp., vol. 11, pp. 48-53, (2003).
24. J. Limpert, T. Schreiber, S. Nolte, H. Zellmer, T. Tunnermann, R. Iliew, F. Lederer, J. Broeng, G. Vienne, A. Petersson, and C. Jakobsen, “High power air 107 clad large-mode-area photonic crystal fiber laser,” Opt. Exp., vol. 11, pp. 818–823, (2003).
25. J. C. Baggett, T. M. Monro, K. Furusawa, and D. J. Richardson, “Comparative study of large-mode holey and conventional fibers,” Opt. Lett., vol. 26, pp. 1045-1047, (2001).
26. J. R. Folkenberg, M. D. Nielsen, N. A. Mortensen, C. Jakobsen, and H. R. Simonsen, “Polarization maintaining large mode area photonic crystal fiber,” Opt. Exp., vol. 12, pp. 956-960, (2004).

27. K. Li, Y. Wang, W. Zhao, G. Chen, Q. Peng, D. Cui, and Z. Xu, “High power single-mode large-mode-area photonic crystal fiber laser with improved Fabry-Perot cavity,” Chin. Opt. Lett., vol. 4, pp. 522-524, (2006).
28. V. Rastogi and K. S. Chiang, “Leaky optical fiber for large mode area single mode operation,” Electron. Lett., vol. 39, pp. 1110-1112, (2003).
29. M. R. Ramadas, E. Garmire, A. K. Ghatak, K. Thyagarajan and M. R. Shenoy, “Analysis of absorbing and leaky planar waveguide: a novel method,” Opt. Lett., vol. 14, pp. 376-378, (1989).
30. K. S. Chiang, “Dual effective-index method for the analysis of rectangular dielectric waveguides,” Appl. Opt., vol. 25, pp. 2169-2174, (1986).
31. B. M. A. Rahman and J. B. Davies, “Finite-element solution of integrated optic waveguides,” J. Lightwave Technol., vol. 2, pp. 682-688, (1984).
32. M. Koshiba and K. Saitoh, “Finite element analysis of birefringence and dispersion properties in actual and idealized holey-fiber structures,” Appl. Opt., vol. 42, pp. 6267-6275, (2003).